Biochem. J. (2013) **456**, 99–108 (Printed in Great Britain) doi:10.1042/BJ20130123

Ribonucleases as a host-defence family: evidence of evolutionarily conserved antimicrobial activity at the N-terminus

Marc TORRENT*†[1,2], David PULIDO*[1], Javier VALLE†, M. Victòria NOGUÉS*, David ANDREU†[2] and Ester BOIX*[2]

*Department of Biochemistry and Molecular Biology, Universitat Autònoma de Barcelona, Cerdanyola del Vallès, 08193 Barcelona, Spain, and †Department of Experimental and Health Sciences, Universitat Pompeu Fabra, Dr. Aiguader 88, 08003 Barcelona, Spain

Vertebrate secreted RNases (ribonucleases) are small proteins that play important roles in RNA metabolism, angiogenesis or host defence. In the present study we describe the antimicrobial properties of the N-terminal domain of the hcRNases (human canonical RNases) and show that their antimicrobial activity is well conserved among their lineage. Furthermore, all domains display a similar antimicrobial mechanism, characterized by bacteria agglutination followed by membrane permeabilization. The results of the present study show that, for all antimicrobial hcRNases, (i) activity is retained at the N-terminus and (ii) the antimicrobial mechanism is conserved. Moreover, using computational analysis we show that antimicrobial propensity may be conserved at the N-terminus for all vertebrate RNases, thereby suggesting that a defence mechanism could be a primary function in vertebrate RNases and that the N-terminus was selected to ensure this property. In a broader context, from the overall comparison of the peptides' physicochemical and biological properties, general correlation rules could be drawn to assist in the structure-based development of antimicrobial agents.

Key words: antimicrobial peptide, drug discovery, evolution, innate immunity, ribonuclease.

INTRODUCTION

RNase (ribonuclease) A-homologues comprise a vertebrate-specific superfamily that includes a wide network of diverse gene lineages [1]. Eight human members (known as canonical RNases) belong to the RNase A-like family [2,3]. They are all small secreted proteins (approximately 15 kDa), sharing a typical fold, with six or eight cysteine residues arranged in three or four disulfide bonds [4–9]. All RNases include a conserved catalytic triad comprising two histidine residues and one lysine residue, the latter located inside the characteristic RNase signature (CKXXNTF) [2] (Supplementary Figure S1 at http://www.biochemj.org/bj/456/bj4560099add.htm).

All hcRNases (human canonical RNases) are catalytically active in variable degrees [10] and some of them share relevant antimicrobial properties [11]. However, antimicrobial and catalytic activities of hcRNases are apparently unrelated [9,11,12]. In particular, studies in zebrafish [13] and chicken RNases [14] show they display antimicrobial properties independent of a catalytic activity. Interestingly, vertebrate RNases have high isoelectric points, a common feature in antimicrobial proteins, required for interaction with the negatively charged membranes of pathogens [11,15].

In summary, the presence of antimicrobial activity in diverse lineages of vertebrate RNases suggests that host defence might be a relevant physiological role of the superfamily [16]. However, a sequential or structural evolutionarily selected pattern that embodies the antimicrobial activity has not yet been reported.

In this context, we previously described that, for RNase 3, a functional antimicrobial domain is located at the N-terminus of the protein [17–20]. This domain can be further dissected into two active regions: (i) residues 24–45 are essential for the antimicrobial action, and (ii) residues 8–16 contribute to agglutination and membrane destabilization [17].

Given that many RNases display antimicrobial properties unrelated to their ribonuclease activity, it is appealing to hypothesize that an N-terminal antimicrobial domain could be preserved and/or refined along evolution to embody the antimicrobial activity. To test this hypothesis, we have synthesized the N-terminal domains of all hcRNases and studied their antimicrobial properties. The results of the present study reveal that (i) antimicrobial activity is largely confined at the N-terminus, and that (ii) the mechanism of action of the N-terminal domains is similar to that of the original proteins. Moreover, complementary computational analyses suggest that the N-terminal domain in the protein might have been selected by evolution to provide a host-defence function.

MATERIALS AND METHODS

Materials and strains

DOPC (1,2-dioleoyl-*sn*-glycero-3-phosphocholine) and DOPG (1,2-dioleoyl-*sn*-glycero-3-phosphoglycerol) were from Avanti Polar Lipids. LPS (lipopolysaccharide) from *Escherichia coli* was purchased from Sigma–Aldrich.

ANTS (8-aminonaphthalene-1,3,6-trisulfonic acid), DPX (*p*-xylenebispyridinium bromide), BC [BODIPY® cadaverine, where BODIPY is boron dipyrromethene (4,4-difluoro-4-bora-3a,4a-diaza-*s*-indacene)] and SYTOX were purchased from

Abbreviations used: ACN, acetonitrile; ANTS, 8-aminonaphthalene-1,3,6-trisulfonic acid; BC, BODIPY® cadaverine; DIEA, *N*,*N*-di-isopropylethylamine; DLS, dynamic light scattering; DOPC, 1,2-dioleoyl-*sn*-glycero-3-phosphocholine; DOPG, 1,2-dioleoyl-*sn*-glycero-3-phosphoglycerol; DPX, *p*-xylenebispyridinium bromide; HBTU, 2-(1*H*-benzotriazol-1-yl)-1,1,3,3-tetramethyluronium hexafluorophosphate; hcRNase, human canonical ribonuclease; hRNase, human ribonuclease; LPS, lipopolysaccharide; LUV, large unilamellar vesicle; MAC, minimal agglutination concentration; MIC, minimal inhibitory concentration; RBC, red blood cell; RNase, ribonuclease; TFA, trifluoroacetic acid.

[1] These authors contributed equally to this work.
[2] Correspondence may be addressed to any of these authors (email marc.torrent@uab.cat, david.andreu@upf.edu or ester.boix@uab.cat).

Invitrogen. pET11 expression vector and *E. coli* BL21(DE3) cells were from Novagen.

Strains used were *E. coli* (BL2, Novagen), *Staphylococcus aureus* (A.T.C.C. 502A), *Acinetobacter baumannii* (A.T.C.C. 15308), *Pseudomonas* sp (A.T.C.C. 15915), *Micrococcus luteus* (A.T.C.C. 7468) and *Enterococcus faecium* (A.T.C.C. 19434).

Peptide synthesis

Fmoc-protected amino acids and HBTU [2-(1*H*-benzotriazol-1-yl)-1,1,3,3-tetramethyluronium hexafluorophosphate] were obtained from Iris Biotech. Fmoc-Rink-amide (MBHA) resin was from Novabiochem. HPLC-grade ACN (acetonitrile) and peptide-synthesis-grade DMF (dimethylformamide), DIEA (*N*,*N*-di-isopropylethylamine) and TFA (trifluoroacetic acid) were from Carlo Erba-SDS.

Solid-phase peptide synthesis was done by Fmoc-based chemistry on Fmoc-Rink-amide (MBHA) resin (0.1 mmol) in a model 433 synthesizer (Applied Biosystems) running FastMoc protocols. Couplings used an 8-fold molar excess each of Fmoc-amino acid and HBTU and a 16-fold molar excess of DIEA. Side chains of trifunctional residues were protected with t-butyl (aspartate, glutamate, serine, threonine and tyrosine), t-butyloxycarbonyl (lysine and tryptophan), 2,2,4,6,7-pentamethyldihydrobenzofuran-5-sulfonyl (arginine) and trityl (asparagine, glutamine and histidine) groups. After chain assembly, full deprotection and cleavage were carried out with TFA/water/tri-isopropylsilane (95:2.5:2.5, by vol.) for 90 min at room temperature (25 °C). Peptides were isolated by precipitation with ice-cold diethyl ether and separated by centrifugation (3000 ***g*** for 20 min at 4 °C), dissolved in 0.1 M acetic acid, and freeze-dried. Analytical reversed-phase HPLC was performed on a Luna C_{18} column (4.6 mm×50 mm, 3 μm; Phenomenex). Linear 5–60 % gradients of solvent B (0.036 % TFA in ACN) into solvent A (0.045 % TFA in water) were used for elution at a flow rate of 1 ml/min and with UV detection at 220 nm. Preparative HPLC runs were performed on a Luna C_{18} column (21.2 mm×250 mm, 10 μm; Phenomenex), using linear gradients of solvent B (0.1 % in ACN) into solvent A (0.1 % TFA in water), as required, with a flow rate of 25 ml/min. MALDI–TOF mass spectra were recorded in the reflector or linear mode in a Voyager DE-STR workstation (Applied Biosystems) using an α-hydroxycinnamic acid matrix. Fractions of adequate (> 90 %) HPLC homogeneity and with the expected mass were pooled, freeze-dried and used in subsequent experiments.

MIC (minimal inhibitory concentration) and MAC (minimal agglutination concentration) determinations

Antimicrobial activity was expressed as the MIC_{100}, defined as the lowest protein concentration that completely inhibits microbial growth. The MIC of each peptide was determined from two independent experiments performed in triplicate for each concentration. Bacteria were incubated at 37 °C overnight in LB broth and diluted to give approximately 5×10^5 CFU (colony-forming units)/ml. The bacterial suspension was incubated with peptides at various concentrations (0.1–10 μM) at 37 °C for 4 h in phosphate buffer. Samples were plated on to Petri dishes and incubated at 37 °C overnight.

For MAC determination, bacterial cells were grown at 37 °C to mid-exponential phase ($D_{600} = 0.6$), centrifuged at 5000 ***g*** for 2 min, and resuspended in LB to give an absorbance of 0.2 at 600 nm. A 200 μl aliquot of the bacterial suspension was incubated with peptides at various (0.1–10 μM) concentrations at 25 °C for 4 h. Aggregation behaviour was observed by visual inspection and the MAC was expressed as described previously [20].

Haemolytic activity

Fresh sheep RBCs (red blood cells) (Oxoid) were washed three times with PBS [35 mM phosphate buffer and 0.15 M NaCl (pH 7.4)] by centrifugation for 5 min at 3000***g*** and resuspended in PBS at 2×10^7 cells/ml. RBCs were incubated with peptides at 37 °C for 4 h and centrifuged at 13000 ***g*** for 5 min. The supernatant was separated from the pellet and its absorbance measured at 570 nm. T100 % haemolysis was defined as the absorbance obtained by sonicating RBCs for 10 s. HC_{50} was calculated by fitting the data to a sigmoidal function.

FACS assay

Bacterial cells were grown at 37 °C to mid-exponential phase ($D_{600} = 0.6$), centrifuged at 5000 ***g*** for 2 min, resuspended in 10 mM sodium phosphate buffer and 100 mM NaCl (pH 7.4) to give a final $D_{600} = 0.2$ and pre-incubated for 20 min. A 500 μl aliquot of the bacterial suspension was incubated with 5 μM peptide for 4 h. After incubation, 25000 cells were subjected to FACS analysis using a FACSCalibur cytometer (BD Biosciences) and a dot-plot was generated by representing the low-angle forward scattering (FSC-H) in the *x*-axis and the side scattering (SSC-H) in the *y*-axis to analyse the size and complexity of the cell cultures. Results were analysed using FlowJo (Tree Star).

LUV (large unilamellar vesicle) liposome preparation

LUVs containing DOPC, DOPG or DOPC/DOPG (3:2 molar ratio) of a defined size (approximately 100 nm) were prepared as described previously [21]. LUVs were obtained from a vacuum-drying lipid chloroform solution by extrusion through 100 nm polycarbonate membranes. The lipid suspension was frozen and thawed ten times before extrusion. A 1 mM stock solution of liposome suspension in 10 mM phosphate buffer and 100 mM NaCl (pH 7.4) was prepared.

Liposome leakage assay

The ANTS/DPX liposome leakage fluorescence assay was performed as described previously [21]. Briefly, a unique population of LUVs of DOPC/DOPG (3:2 molar ratio) lipids was obtained containing 12.5 mM ANTS, 45 mM DPX, 20 mM NaCl and 10 mM Tris/HCl (pH 7.4). The ANTS/DPX liposome suspension was diluted to a 30 μM concentration and incubated at 25 °C in the presence of peptide. Leakage activity was followed by monitoring the increase in fluorescence at 535 nm [22].

Liposome agglutination assay

Liposome agglutination was analysed by DLS (dynamic light scattering) using a Malvern 4700 photon correlation spectrometer (Malvern Instruments). An argon laser ($\lambda = 488$ nm) was used to cover the wide size range involved. Hydrodynamic radius measurements were always carried out at a reading scattering angle of 90°. From the intensity measurements recorded, data were processed by the CONTIN software (Malvern), and the hydrodynamic diameter, the polydispersity index and the total number of counts were calculated. The incubation buffer was

10 mM Tris/HCl and 100 mM NaCl (pH 7.4). Measurements were performed at 25 °C, a 200 μM final liposome concentration, and a 5 μM peptide concentration.

LPS-binding assay

LPS binding was assessed using the fluorescent probe BC as described previously [23]. Briefly, the displacement assay was performed by adding 1–2 μl aliquots of peptide to 1 ml of a continuously stirred mixture of LPS (10 μg/ml) and BC (10 μM) in 10 mM phosphate buffer and 100 mM NaCl (pH 7.5). Fluorescence measurements were performed on a Cary Eclipse spectrofluorimeter, with 580 and 620 nm as BC excitation and emission wavelengths respectively. The excitation slit was set at 2.5 nm, and the emission slit was set at 20 nm. Final values correspond to an average of four replicates and were the mean of a 0.3 s continuous measurement. Occupancy factor was calculated as described previously [23].

CD spectroscopy

Far-UV CD spectra were recorded in a Jasco J-715 spectropolarimeter as described previously [24]. Mean-residue ellipticity $[\theta]$ (deg·cm^2·dmol^{-1}) was calculated as

$$[\theta] = \frac{\theta(\mathrm{MRW})}{10cl}$$

where θ is the experimental ellipticity (deg), MRW is the mean residue molecular mass of the peptide, c is the molar concentration of peptide and l is the cell path length. Data from four consecutive scans were averaged. Spectra of peptides [4–8 μM in 5 mM sodium phosphate (pH 7.5)] in the absence and presence (1 mM) of SDS and LPS (1 mM, nominal molecular mass = 90 kDa) were recorded. Samples were centrifuged for 5 min at 10000 ***g*** before use.

SYTOX Green uptake

For SYTOX Green assays, bacterial *E. coli* and *S. aureus* cells were grown to mid-exponential growth phase (D_{600}~0.6) in LB medium and then centrifuged (5000 ***g*** for 2 min at 25 °C), washed and resuspended in phosphate buffer. Cell suspensions (D_{600}~0.2) were incubated with 1 μM SYTOX Green (Invitrogen) for 15 min in the dark before the influx assay. At 2–4 min after initiating data collection, 5 μM peptide was added to the cell suspension, and the increase in SYTOX Green fluorescence was measured (485 and 520 nm excitation and emission wavelengths respectively) for 40 min in a Cary Eclipse spectrofluorimeter. Maximum fluorescence was that resulting from cell lysis with Triton X-100.

Bacterial cytoplasmic membrane depolarization assay

Membrane depolarization was monitored as described previously [25]. Briefly, *E. coli* and *S. aureus* strains were grown at 37 °C to an D_{600} of 0.2, centrifuged at 5000 ***g*** for 7 min, washed with 5 mM Hepes (pH 7.2) containing 20 mM glucose and resuspended in 5 mM Hepes-KOH, 20 mM glucose and 100 mM KCl (pH 7.2) to an D_{600} of 0.05. DiSC3(5) (3,3-dipropylthiadicarbocyanine iodide) was added to a final concentration of 0.4 μM, and changes in the fluorescence were continuously recorded after the addition of peptide (5 μM). The concentration required to achieve half of total membrane depolarization was estimated from non-linear regression analysis.

RESULTS

Design of hcRNase-derived peptides

As the reference 1–45 segment in hcRNase 3 has been found to be the minimal domain retaining full antimicrobial properties [20,24], in a search for similar antimicrobial properties, peptides **1**–**8**, comprising equivalent regions of other RNase N-termini [residues 1–45 of hRNases (human RNases) 2, 6, 7 and 8; residues 1–48 of hRNases 1 and 4; and residues 1–47 of RNase 5; Table 1] were selected for synthesis. In all cases, the peptides included the first two α-helices as well as the first β-strand from the parental protein. As described previously [12], the two cysteine residues in the N-terminal region, disulfide-linked to a distant cysteine residue in the native protein, were replaced by isosteric serine residues. Peptides of satisfactory quality, with the expected molecular mass, were obtained after Fmoc solid-phase synthesis and HPLC purification (Table 1). Their CD secondary structures in the presence of structuring agents [TFE (trifluoroethanol) and DPC (dodecylphosphocholine) micelles] were found to be similar to those of the cognate proteins [24,26].

Antimicrobial activity of hcRNases is retained at the N-terminus

To assess the antimicrobial activity of peptides **1**–**8** we determined their MIC for three representative Gram-negative and Gram-positive bacteria (Table 2). Five peptides (**1**, **3**, **4**, **6** and **7**) tested active against all strains, with MIC values between 0.2 and 10 μM, a range close to that observed for several hcRNases [9,17,24]. In contrast, peptides **2**, **5** and **8** were inactive against all strains. When these results are compared with available literature data on hcRNases, a good agreement between the two sets of data is observed (Table 2), with only peptide **8** differing from previously reported results [27]. As we suspected that the discrepancy observed could be due to the inoculum size (5×10^5 cells/ml in our case, 5×10^4 cells/ml in Rudolph et al. [27]), peptide **8** was reassayed using a 5×10^4 cells/ml inoculum and MIC values in the 1–10 μM range, compatible with the previous report [27], were determined. Thus we conclude that the antimicrobial activity of hcRNases is consistently preserved at the N-terminus.

To characterize the cell selectivity of peptides **1**–**8**, their haemolytic activity was tested on sheep RBCs. For antimicrobially active peptides (**1**, **3**, **4** and **6**–**8**), haemolytic activities (measured as HC_{50}) between 10 and 20 μM were found (Table 2), whereas no haemolysis ($HC_{50} > 100$ μM) was detected for antimicrobially inert peptides **2** and **5**. For the most antimicrobially active peptides (**3**, **4**, **6** and **7**) MICs were one or two orders of magnitude lower than HCs, suggesting that hcRNase-derived peptides are good candidates for drug development, as already shown for RNase 3 [20].

The antimicrobial mechanism of hcRNases primarily involves the N-terminus

To characterize the antimicrobial mechanism of hcRNase-derived peptides **1**–**8**, we first assessed their ability to depolarize and permeabilize bacterial cytoplasmic membranes. Results with representative Gram-negative and Gram-positive organisms (Table 3) show that only the peptides with high bactericidal activity (**3**, **4**, **6** and **7**) can cause significant membrane

Table 1 Physicochemical properties of the hcRNase-derived peptides

In every peptide, the underlined serine residue (S) corresponds to cysteine residues in the native protein. Hydrophobicity was computed using the GRAVY scale.

Peptide	Sequence	$[M+H]^+$ Measured mass (Da)	Theoretical mass (Da)	Retention time (min)*	Hydrophobicity	pI
1	---KESRAKKFQRQHMDSDSSPSSSSTYSNQMMRRRNMTQGRSKPVNTFVH	5630.45	5628.72	4.93	− 1.575	11.40
2	KPPQFTWAQWFETQHINMTSQ------QSTNAMQVINNYQRRSKNQNTFLL	5453.32	5452.67	8.56	− 1.069	10.28
3	RPPQFTRAQWFAIQHISLNPP------RSTIAMRAINNYRWRSKNQNTFL	5478.34	5478.74†	5.05†	− 0.764	11.88
4	--QDGMY-QRFLRQHVHPEET-GGSDRYSNLMMQRRKMTLYHSKRFNTFIH	5812.31	5824.84	6.69	− 1.228	10.15
5	--QDNSRYTHFLTQHYDAKPQ-GRDDRYSESIMRRRGLTS-PSKDINTFIH	5638.15	5635.76	6.43	− 1.430	9.40
6	WPKRLTKAHWFEIQHIQPSPL------QSNRAMSGINNYTQHSKHQNTFLH	5410.85	5404.74	6.88	− 1.096	10.45
7	KPKGMTSSQWFKIQHMQPSPQ------ASNSAMKNINKHTKRSKDLNTFLH	5206.90	5205.67	6.20	− 1.209	10.75
8	KPKDMTSSQWFKTQHVQPSPQ------ASNSAMSIINKYTERSKDLNTFLH	5206.95	5204.59	7.48	− 1.044	9.70

*All peptides except RNase 3 were analysed as described in the Materials and methods section. For RNase 3, data are from [12].
†Data from [12]; HPLC as described in the Materials and methods section, except that the gradient was 20–45 % solvent B into solevnt A over 15 min.

Table 2 Antimicrobial and haemolytic activities of the hcRNase N-terminal peptides

n.r., not reported (antimicrobial activity has not been assayed for some proteins).

	Antimicrobial activity MIC_{100} (μM)							Haemolytic activity HC_{50} (μM)
	Gram-negative bacteria			Gram-positive bacteria				
Peptide	*E. coli*	*P. aeruginosa*	*A. baumanii*	*S. aureus*	*M. luteus*	*E. faecium*	Protein antimicrobial activity*	Sheep RBCs
1	9	9	9	5	9	5	n.r.	11.6
2	> 10	> 10	> 10	> 10	> 10	10	−	> 100
3	0.4	0.4	0.3	0.5	0.6	0.6	+ + +	9.5
4	0.3	0.4	0.5	0.3	1.2	0.8	n.r.	15.2
5	> 10	> 10	> 10	> 10	> 10	> 10	−	> 100
6	1.2	1.2	1.2	5	2.5	2.5	n.r.	17.4
7	1.2	1.2	1.2	10	5	2.5	+ + +	10.4
8	> 10	10	> 10	> 10	> 10	> 10	+	15.1

*Antimicrobial activity of the parental proteins obtained from [17].

Table 3 Depolarization and bacteria leakage IC_{50} values for hcRNase-derived peptides

Peptide	Depolarization (nM)		Bacteria leakage (nM)	
	E. coli	*S. aureus*	*E. coli*	*S. aureus*
1	150 ± 10	350 ± 13	> 10	9.1 ± 1
2	> 1000	> 1000	> 10	> 10
3	40 ± 1	50 ± 7	3.8 ± 0.1	4.5 ± 0.5
4	40 ± 3	30 ± 2	3.8 ± 0.2	6.1 ± 0.1
5	> 1000	> 1000	> 10	> 10
6	40 ± 4	40 ± 2	5.0 ± 0.3	7.3 ± 0.7
7	40 ± 3	70 ± 1	5.7 ± 0.1	7.3 ± 0.2
8	> 1000	> 1000	> 10	> 10

Table 4 LPS affinity, agglutination activity and liposome leakage of hcRNase-derived peptides

Values are expressed as ED_{50}. n.d., not detected at the assayed concentration range (0.1–10 μM).

Peptide	LPS binding (μM)	MAC* (μM)	Liposome leakage (nM)		
			DOPC	DOPC/DOPG	DOPG
1	5.6 ± 1.3	5.0 ± 0.5	> 1000	> 1000	206 ± 77
2	7.1 ± 1.0	n.d.	> 1000	> 1000	> 1000
3	2.9 ± 0.3	0.9 ± 0.1	> 1000	95 ± 5	99 ± 2
4	1.3 ± 0.2	5.0 ± 0.5	> 1000	580 ± 10	53 ± 5
5	n.d.	n.d.	> 1000	> 1000	> 1000
6	1.9 ± 0.3	1.8 ± 0.1	> 1000	210 ± 30	86 ± 10
7	3.2 ± 1.2	5 ± 0.5	> 1000	180 ± 20	108 ± 4
8	n.d.	n.d.	> 1000	> 1000	> 1000

*MAC values obtained with *E. coli* cultures.

depolarization and permeabilization, in agreement with the antimicrobial values (Table 2).

Another specific characteristic of antimicrobial proteins, already demonstrated for the N-terminal domain of hcRNase 3 (peptide **3**) [12,15], is the ability to agglutinate Gram-negative bacteria, judged as important in holding pathogens at bay at the infection focus. To test whether other hcRNase-derived peptides shared this property, their MAC was determined (Table 4). Interestingly, all antimicrobially active peptides (**1**, **3**, **4**, **6** and **7**) showed agglutinating properties to a certain degree, suggesting that this antimicrobial feature is conserved for all hcRNases. Furthermore, MAC values correlated well with LPS-binding affinities (Table 4 and Supplemenatry Table S1 at http://www.biochemj.org/bj/456/bj4560099add.htm), suggesting that binding to the Gram-negative bacterial cell wall would trigger the agglutinating mechanism, as described previously [27a]. In agreement with this, no agglutination was observed for Gram-positive *S. aureus*, confirming the fact that an LPS external layer is necessary for bacterial agglutination. To further explore these agglutinating properties, we used FACS. After incubation of *E. coli* cell cultures with the hcRNase-derived peptides, significant

agglutination was only observed for active peptides **1**, **3**, **4**, **6** and **7** (Figure 1A), with peptide **3**, followed by **6**, displaying the highest activity. Additionally, bacterial cells were incubated with SYTO9 and propidium iodide to assess their viability simultaneously with agglutination (Figure 1B). Results showed dead bacteria to be present only when significant agglutinating activity was also detected, suggesting that both activities are part of a sole mechanism. One may therefore generalize the behaviour of all active hcRNase-derived peptides as having the ability to dock on to external LPS layers and promote Gram-negative bacteria agglutination, triggering, in turn, membrane depolarization and lipid bilayer leakage, eventually resulting in cell death. For Gram-positive cells, peptides would probably diffuse across the permeable cell wall and exert their lytic action on to the cell membrane [25].

Previously we showed that the hcRNase 3 N-terminal domain (peptide **3**) retains the ability of the cognate protein to bind and disrupt model membranes [20,24]. To determine whether all hcRNase-derived peptides behave similarly, we studied the effect of the peptides on lipid bilayer models. Changes in the tryptophan spectrum upon incubation with liposomes, a usual readout for membrane interaction, could only be assessed for peptides bearing this residue (**2**, **3**, **6**, **7** and **8**; Supplementary Table S1), but in all cases showed a good agreement with antimicrobial activity. As reported for many other antimicrobial peptides, hcRNase-derived peptides were able to bind anionic liposomes, whereas no significant binding was observed for neutral ones, suggesting that electrostatic interactions are indispensable for peptide binding to lipid vesicles.

Next, the ability of the peptides to perturb bilayer stability was tested in a liposome leakage assay (Table 4). As expected, only active peptides displayed high leakage activity, and values observed for liposome content release were in good agreement with those observed for depolarization activity in bacteria (Table 3).

For a better characterization of the mechanism, the ability of hcRNase-derived peptides to agglutinate liposomes was studied by DLS, which allows monitoring of the vesicle size. All peptides were tested against both neutral and negatively charged vesicles (Figure 2), but only the latter agglutinated upon peptide interaction, again highlighting the role of electrostatic interactions in promoting agglutination. More interestingly, the only peptides capable of promoting agglutination in this assay with model membranes were those previously found to be active in either MAC or FACS experiments (Table 3 and Figure 1).

As some hcRNases are rich in lysine residues (e.g. RNase 7) while others are rich in arginine residues (e.g. RNase 3) we committed ourselves to test whether the content of arginine or lysine could modulate the mechanism of action of the hcRNases N-termini and synthesized the lysine and arginine variants of peptides **3** and **7** respectively. In all cases, we did not find any significant differences either in the antimicrobial properties of the peptides or in their biophysical properties (Supplementary Table S2 at http://www.biochemj.org/bj/456/bj4560099add.htm). Both variants had identical activities and were able to depolarize and agglutinate bacteria with the same efficiency as their natural partners (Supplementary Table S2). Therefore we conclude that these residues are interchangeable in terms of their contribution to the antimicrobial activities of the N-terminal domain.

In summary, results obtained using model membranes correlated well with those using bacterial cultures, hence reinforcing our hypothesis that bactericidal mechanisms are consistently conserved at the N-termini of antimicrobially active hcRNases.

Vertebrate RNases share a conserved N-terminal antimicrobial domain

A next logical step was to analyse the antimicrobial activity of the N-terminus across vertebrate RNases. To this end, we analysed all RNase A homologues deposited at the Uniprot (http://www.uniprot.org) database using AMPA, an algorithm that scans proteins in search of potential antimicrobial regions (http://tcoffee.crg.cat/apps/ampa/) [15,28]. Results are summarized in Figure 3 in the form of a phylogenetic tree of vertebrate RNases together with AMPA-identified putative antimicrobial regions at the N-termini of these proteins. It can be seen that most of these N-termini are potentially antimicrobial, in congruence with the experimental data in the present study (Table 1). Results in Figure 3, particularly the evolutionary distances among different hcRNases, suggest that N-terminal regions endowed with antimicrobial properties have been central in the function of RNases since their early origins and have accordingly been conserved along evolution.

DISCUSSION

RNases are widely distributed in most vertebrate organs and tissues and can exert many different functions. Interestingly, many members of the RNase A superfamily, not only in mammals but also in other vertebrates, like fish and amphibians [1,14,16], show antimicrobial properties apparently unrelated to their nuclease activity. It has indeed been suggested that RNases might have emerged as a host-defence family in vertebrate evolution [16].

Although the three-dimensional structure of RNase A-like proteins is highly conserved, their amino acid sequence is quite diverse and a defined antimicrobial signature cannot be easily delineated. This is indeed the case for most antimicrobial peptides and proteins, sharing microbicidal properties despite low sequence similarity. Poor sequence homology has in practice prevented the development of robust methods for predicting antimicrobial motifs in proteins and peptides [15,28,29]. However, despite the lack of sequential or structural patterns, similar physicochemical characteristics are shared among antimicrobial peptides, like a net positive charge or the high hydrophobic amino acid content [30].

Previously, we described that the antimicrobial properties of hRNase 3 are highly retained in its N-terminal domain [20,24]. This domain is equipotent compared with the whole protein, killing both Gram-negative and Gram-positive bacteria and retains its biophysical properties, including membrane agglutination and leakage [20,24]. More interestingly, the chemically synthesized antimicrobial domain has a similar structure compared with its counterpart in the native protein in membrane-like environments [26]. However, as pointed out below, there is no significant sequence similarity between the antimicrobial N-terminus of hRNase 3 and those of other antimicrobial RNases (see the Supplementary Online Data and Supplementary Figures S1 and S2 at http://www.biochemj.org/bj/456/bj4560099add.htm). For instance, the residues reported to be critical for antimicrobial activity in hRNases 3 and 7 are not significantly conserved (Supplementary Figure S1) [17]. Nonetheless, all hcRNase N-termini have a high isolectric point and similar hydrophobicity (Table 1).

In the present study, we have shown that all N-terminal antimicrobial domains of hcRNases with described antimicrobial activity are active against both Gram-positive and Gram-negative bacteria (Table 2). Even more interesting, in the cases where enough experimental information on the antimicrobial activity of

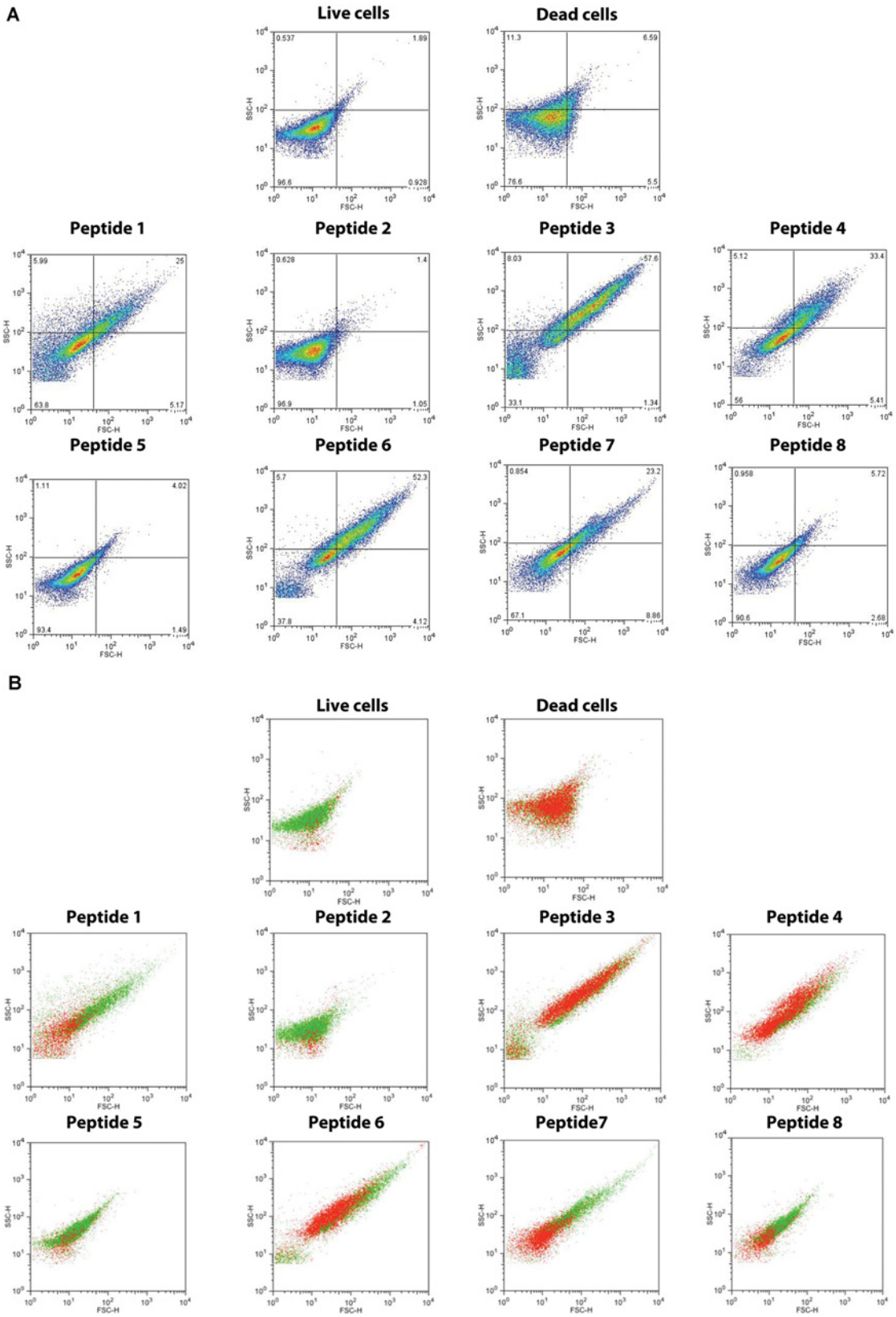

Figure 1 Bacterial agglutination measured by FACS

E. coli cell cultures were incubated with hcRNase-derived peptides at a 5 μM concentration for 4 h and analysed using a FACSCalibur cytometer. Low-angle forward scattering (FSC-H) is represented on the *x*-axis and the side scattering (SSC-H) on the *y*-axis to analyse the size and complexity of the cell cultures. (**A**) Plots are coloured to show cell density. Low (blue) to high (red) cell densities are represented. The percentages of cells belonging to each quadrant are indicated. (**B**) Plots are coloured to show cell viability. Live cells (stained with Syto9, green) and dead cells (stained with propidium iodide, red) are coloured in the plot. Control live and dead cells were analysed as a reference.

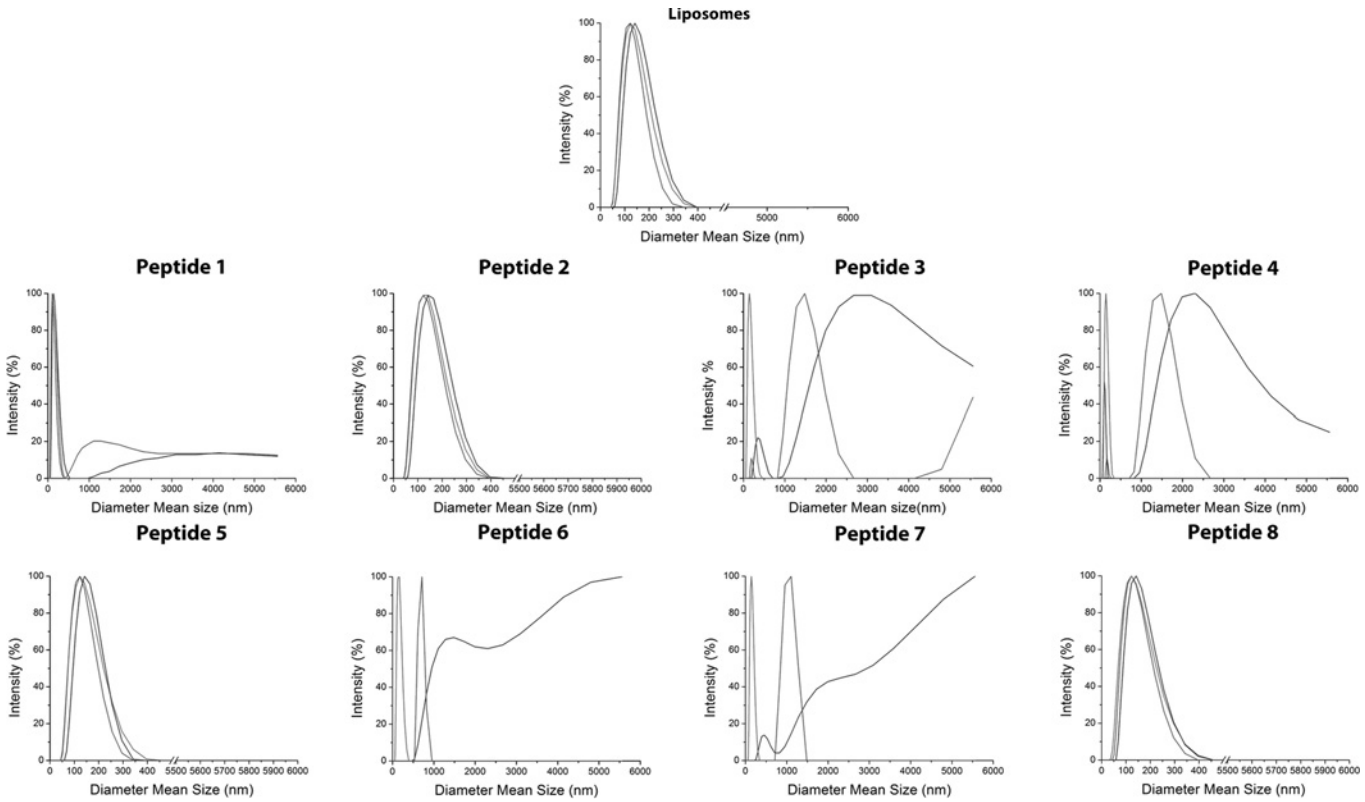

Figure 2 Liposome aggregation measured by DLS

Liposomes containing DOPC (light grey), DOPG (black) or a 3:2 molar mixture of DOPC/DOPG (dark grey) were incubated with 5 μM hcRNase-derived peptides and the size was measured after 15 min by DLS using a Malvern 4700 spectrometer. The plots represent the intensity against the liposome mean size. For peptides **6** and **7** with DOPG liposomes, large aggregates were observed which made it difficult to determine a defined particle mean size.

the proteins is available, the peptides tested have similar activity (Table 2). We have also analysed the biophysical characteristics of the peptides and evaluated the correlation between their ability to disrupt model membranes and their inherent antimicrobial activity (Tables 2 and 3). Liposome leakage shows a good correlation with both antimicrobial activity and membrane depolarization (Supplementary Figure S7 at http://www.biochemj.org/bj/456/bj4560099add.htm). The correspondence between leakage and depolarization is particularly interesting as it suggests that the antimicrobial peptides will eventually promote a disruptive action at the membrane level, rather than interacting with internal targets in the microbes. Interestingly, there is a significant correlation between the ability to acquire a defined structure in membrane-like environments (e.g. SDS micelles) and the antimicrobial activity (Supplementary Figures S6 and S8 at http://www.biochemj.org/bj/456/bj4560099add.htm), suggesting that peptides would adopt an α-helical structure to perturb the bacterial membrane integrity. In fact, all RNases conserve the helical structure at their N-terminus (Supplementary Figure S9 at http://www.biochemj.org/bj/456/bj4560099add.htm).

Indeed, all hcRNase N-terminal peptides with antimicrobial activity show significant agglutination activity, suggesting that this trait might be inherent to antimicrobial RNases. The agglutinating activity of hcRNase 3 has been previously attributed to a high aggregation-prone region at the N-terminus (residues 8–16) [19,25]. Removal of this corresponding hydrophobic patch inside the antimicrobial domain drastically reduces hcRNase 3 antimicrobial activity, particularly in Gram-negative species. A comparison of the computed aggregation propensity profiles of all RNases shows a significant correlation between the aggregation propensity in this particular region and the observed agglutinating activity (Supplementary Figures S3 and S4 at http://www.biochemj.org/bj/456/bj4560099add.htm), strengthening the conclusion that bacterial agglutination may be a characteristic trait of the antimicrobial mechanism of action. Bacterial agglutination activity is also associated with the ability to bind LPS (Table 4). In fact, agglutination has been shown to take place at the external layers of the Gram-negative bacterial cell wall [23,25]. Accordingly, we suggested that following RNase binding to the external layers of Gram-negative bacteria, a slight conformational change in the protein would expose the N-terminal hydrophobic patch to the surface, thereby triggering agglutination by protein–protein interaction. Bacterial agglutination would therefore correlate with the hydrophobic nature of the aggregation-prone region (Supplementary Figure S5). A side-by-side comparison of the two best-studied antimicrobial hcRNases, 3 and 7, corroborate this behaviour, showing that the agglutination potency is far more intense for RNase 3 than for RNase 7 [25]. In this light, it is reasonable to conclude that both hcRNases and their derived peptides will act by a membrane perturbation mechanism, which supports the hypothesis that RNase activity is not required for the antimicrobial action. Notwithstanding, we should also consider that within the context of the whole RNase A family the distinct members would combine their diverse abilities, and among them their catalytic activity, providing a fast and effective multifaceted mechanism to combat pathogens simultaneously at several

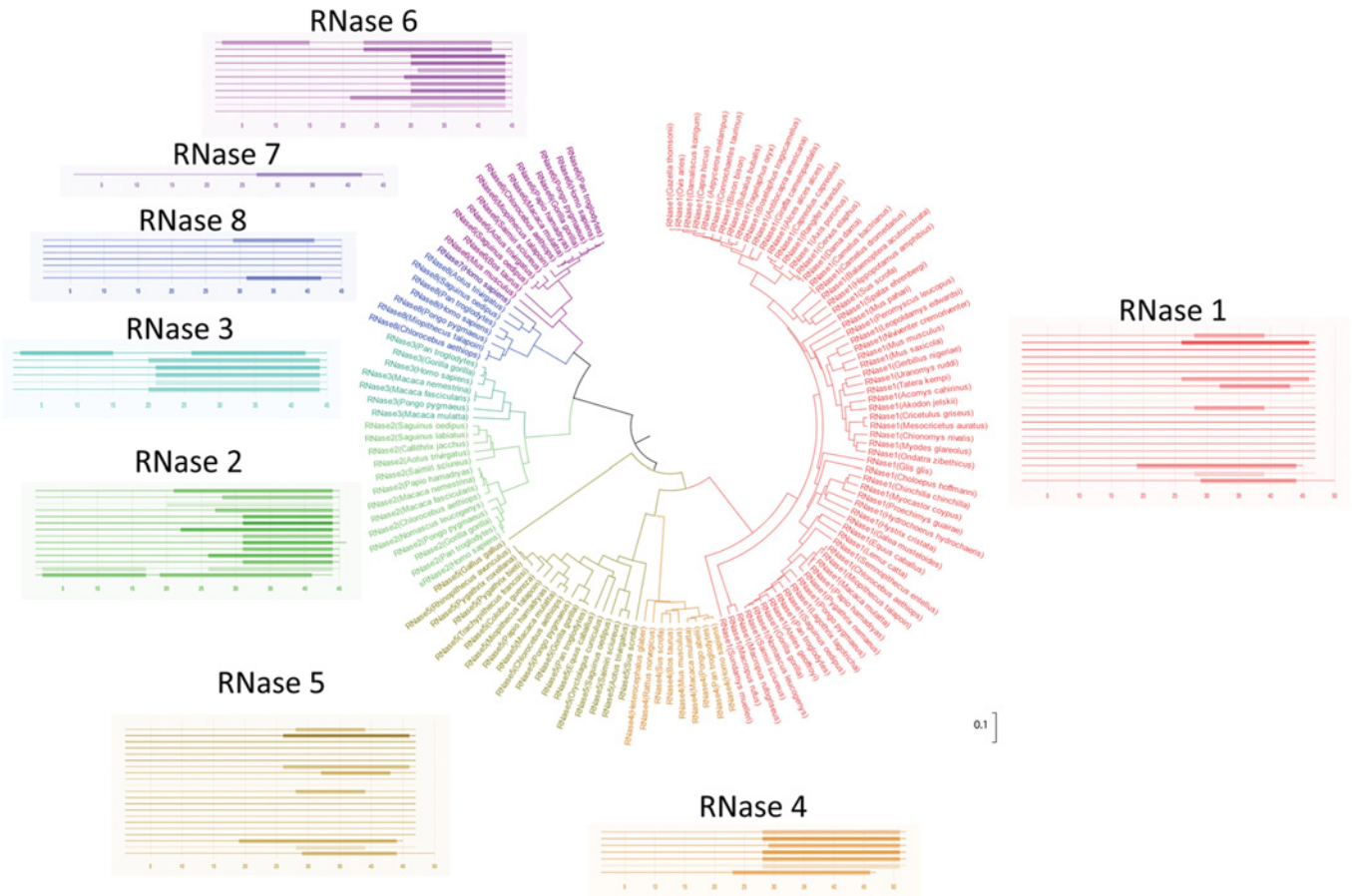

Figure 3 Conservation of the N-terminal antimicrobial domain among vertebrate secreted RNases

The evolutionary history was inferred using the UPGMA method [39]. The optimal tree is shown. The tree is drawn to scale, with branch lengths in the same units as those of the evolutionary distances used to infer the phylogenetic tree. The evolutionary distances were computed using the Poisson distribution method [40] and are in units of number of amino acid substitutions per site. All positions containing gaps and missing data were eliminated. Evolutionary analyses were conducted in MEGA5 [41]. All sequences were analysed using the AMPA algorithm [28]; detected antimicrobial regions in the N-terminal domain are depicted next to the corresponding tree branch. Each type of RNase family is depicted in a different colour.

cellular targets. Indeed, the most recent reviews on antimicrobial peptides point at such a multifunctional working mode [31,32]

Other literature reports also suggest that the N-terminus of RNases might be the main region responsible for their cytotoxicity. For example, Picone and co-workers [33] have found that increasing the positive charge at the N-terminus of bovine seminal RNase enhances membrane interaction and antitumour activity. Interestingly, we have also found comparable behaviours in other cytotoxic RNase families, such as the contribution of the N-terminus of ribotoxin in the interaction with lipid bilayers [34].

The present experimental findings suggest that RNase N-termini might have been selected in evolution to execute host-defence-related functions, particularly those dependent on a cytotoxic action. To strengthen this conclusion, we have analysed the antimicrobial profile of all secreted vertebrate RNases using the AMPA algorithm. The analysis output (Figure 3) shows that most RNases have putative antimicrobial domains at the N-terminal region whose sequences overlap with the antimicrobial-prone region described for hcRNase 3. It is thus reasonable to suggest that both antimicrobial and catalytic activities in the RNase A-like superfamily have evolved independently and that evolution has used the N-terminal domain of RNases to develop anti-pathogen properties. Hence, the results of the present study support the hypothesis that RNases might have emerged as a host-defence family.

Unavoidably, the question about the role of the C-terminal part of the protein remains and has only been partially addressed until now. Although previous studies discard a primary contribution of the C-terminus in the protein bactericidal activity [18,35], we cannot disregard the fact that the active site architecture, shared by all family members, consists of both N- and C-termini. Moreover, residues all along the protein surface are involved in the recognition of the RNA polymer, as identified in some family members studied [36–38]. In this context, one may speculate on an evolutionary constraint to retain those residues implied in the RNA recognition, which could partially account for the differences observed in RNases in terms of catalytic activity [36]. Therefore further investigations are required to provide a complete scenario of the role of the distinct protein domains and their potential contribution in complementary tasks that may prove physiologically relevant.

In conclusion, we have shown that the antimicrobial properties of human RNases are retained in their N-terminal domain. Despite the low sequence conservation, the latent antimicrobial properties of this N-terminal domain in many RNase homologues suggest that this region might have evolved to provide host-defence functions for the protein. In this regard, antimicrobial RNases, and more specifically their N-terminal domains, would therefore constitute suitable scaffolds useful as lead templates for the development of wide-spectrum antibiotics.

AUTHOR CONTRIBUTION

Marc Torrent, Ester Boix and David Andreu conceived and designed the experiments. Javier Valle synthesized the peptides. Marc Torrent and David Pulido performed the experiments. Marc Torrent, David Pulido, M. Victòria Nogués, David Andreu and Ester Boix analysed the data. M. Victòria Nogués, David Andreu and Ester Boix contributed reagents, materials and analysis tools. Marc Torrent, David Andreu and Ester Boix wrote the paper.

FUNDING

This work was supported by the European Union [grant number HEALTH-F3-2008-223414], the Ministerio de Ciencia e Innovación [grant numbers BIO2008-04487-CO3-02, BFU2009-09371, FEDER funds], the Ministerio de Economía y Competitividad [grant number BFU2012-38965] and the Generalitat de Catalunya [grant numbers SGR2009-494, SGR2009-795]. M.T. is a recipient of a Beatriu de Pinós fellowship. D.P. is a recipient of an FPU fellowship (MICINN; Ministerio de Ciencia e Innovación). Microscopy experiments were carried out at the Servei de Microscòpia (Universitat Autònoma de Barcelona) and fluorescence measurements at the Servei d'Anàlisi i Fotodocumentació (Universitat Autònoma de Barcelona). The funders had no role in study design, data collection and analysis, decision to publish, or preparation of the paper.

REFERENCES

1 Dyer, K. D. and Rosenberg, H. F. (2006) The RNase a superfamily: generation of diversity and innate host defense. Mol. Diversity **10**, 585–597
2 Sorrentino, S. (2010) The eight human "canonical" ribonucleases: molecular diversity, catalytic properties, and special biological actions of the enzyme proteins. FEBS Lett. **584**, 2194–2200
3 Cho, S., Beintema, J. J. and Zhang, J. (2005) The ribonuclease A superfamily of mammals and birds: identifying new members and tracing evolutionary histories. Genomics **85**, 208–220
4 Kover, K. E., Bruix, M., Santoro, J., Batta, G., Laurents, D. V. and Rico, M. (2008) The solution structure and dynamics of human pancreatic ribonuclease determined by NMR spectroscopy provide insight into its remarkable biological activities and inhibition. J. Mol. Biol. **379**, 953–965
5 Mosimann, S. C., Newton, D. L., Youle, R. J. and James, M. N. (1996) X-ray crystallographic structure of recombinant eosinophil-derived neurotoxin at 1.83 Å resolution. J. Mol. Biol. **260**, 540–552
6 Laurents, D. V., Bruix, M., Jimenez, M. A., Santoro, J., Boix, E., Moussaoui, M., Nogués, M. V. and Rico, M. (2009) The ^{1}H, ^{13}C, ^{15}N resonance assignment, solution structure, and residue level stability of eosinophil cationic protein/RNase 3 determined by NMR spectroscopy. Biopolymers **91**, 1018–1028
7 Terzyan, S. S., Peracaula, R., de Llorens, R., Tsushima, Y., Yamada, H., Seno, M., Gomis-Rüth, F. X. and Coll, M. (1999) The three-dimensional structure of human RNase 4, unliganded and complexed with d(Up), reveals the basis for its uridine selectivity. J. Mol. Biol. **285**, 205–214
8 Acharya, K. R., Shapiro, R., Allen, S. C., Riordan, J. F. and Vallee, B. L. (1994) Crystal structure of human angiogenin reveals the structural basis for its functional divergence from ribonuclease. Proc. Natl. Acad. Sci. U.S.A. **91**, 2915–2919
9 Huang, Y. C., Lin, Y. M., Chang, T. W., Wu, S. J., Lee, Y. S., Chang, M. D., Chen, C., Wu, S. H. and Liao, Y. D. (2007) The flexible and clustered lysine residues of human ribonuclease 7 are critical for membrane permeability and antimicrobial activity. J. Biol. Chem. **282**, 4626–4633
10 Sorrentino, S. and Libonati, M. (1997) Structure–function relationships in human ribonucleases: main distinctive features of the major RNase types. FEBS Lett. **404**, 1–5
11 Boix, E. and Nogues, M. V. (2007) Mammalian antimicrobial proteins and peptides: overview on the RNase A superfamily members involved in innate host defence. Mol. BioSyst. **3**, 317–335
12 Rosenberg, H. F. (1995) Recombinant human eosinophil cationic protein. Ribonuclease activity is not essential for cytotoxicity. J. Biol. Chem. **270**, 7876–7881
13 Pizzo, E., Varcamonti, M., Di Maro, A., Zanfardino, A., Giancola, C. and D'Alessio, G. (2008) Ribonucleases with angiogenic and bactericidal activities from the Atlantic salmon. FEBS J. **275**, 1283–1295
14 Nitto, T., Dyer, K. D., Czapiga, M. and Rosenberg, H. F. (2006) Evolution and function of leukocyte RNase A ribonucleases of the avian species, *Gallus gallus*. J. Biol. Chem. **281**, 25622–25634
15 Torrent, M., Nogues, V. M. and Boix, E. (2009) A theoretical approach to spot active regions in antimicrobial proteins. BMC Bioinf. **10**, 373
16 Cho, S. and Zhang, J. (2007) Zebrafish ribonucleases are bactericidal: implications for the origin of the vertebrate RNase A superfamily. Mol. Biol. Evol. **24**, 1259–1268
17 Boix, E., Salazar, V. A., Torrent, M., Pulido, D., Nogues, M. V. and Moussaoui, M. (2012) Structural determinants of the eosinophil cationic protein antimicrobial activity. Biol. Chem. **393**, 801–815
18 Sanchez, D., Moussaoui, M., Carreras, E., Torrent, M., Nogues, V. and Boix, E. (2011) Mapping the eosinophil cationic protein antimicrobial activity by chemical and enzymatic cleavage. Biochimie **93**, 331–338
19 Torrent, M., Odorizzi, F., Nogues, M. V. and Boix, E. (2010) Eosinophil cationic protein aggregation: identification of an N-terminus amyloid prone region. Biomacromolecules **11**, 1983–1990
20 Torrent, M., Pulido, D., de la Torre, B. G., Garcia-Mayoral, M. F., Nogues, M. V., Bruix, M., Andreu, D. and Boix, E. (2011) Refining the eosinophil cationic protein antibacterial pharmacophore by rational structure minimization. J. Med. Chem. **54**, 5237–5244
21 Torrent, M., Cuyas, E., Carreras, E., Navarro, S., Lopez, O., de la Maza, A., Nogués, M. V., Reshetnyak, Y. K. and Boix, E. (2007) Topography studies on the membrane interaction mechanism of the eosinophil cationic protein. Biochemistry **46**, 720–733
22 Torrent, M., Sanchez, D., Buzon, V., Nogues, M. V., Cladera, J. and Boix, E. (2009) Comparison of the membrane interaction mechanism of two antimicrobial RNases: RNase 3/ECP and RNase 7. Biochim. Biophys. Acta **1788**, 1116–1125
23 Torrent, M., Navarro, S., Moussaoui, M., Nogues, M. V. and Boix, E. (2008) Eosinophil cationic protein high-affinity binding to bacteria-wall lipopolysaccharides and peptidoglycans. Biochemistry **47**, 3544–3555
24 Torrent, M., de la Torre, B. G., Nogues, V. M., Andreu, D. and Boix, E. (2009) Bactericidal and membrane disruption activities of the eosinophil cationic protein are largely retained in an N-terminal fragment. Biochem. J. **421**, 425–434
25 Torrent, M., Badia, M., Moussaoui, M., Sanchez, D., Nogues, M. V. and Boix, E. (2010) Comparison of human RNase 3 and RNase 7 bactericidal action at the Gram-negative and Gram-positive bacterial cell wall. FEBS J. **277**, 1713–1725
26 Garcia-Mayoral, M. F., Moussaoui, M., de la Torre, B. G., Andreu, D., Boix, E., Nogues, M. V., Rico, M., Laurents, D. V. and Bruix, M. (2010) NMR structural determinants of eosinophil cationic protein binding to membrane and heparin mimetics. Biophys. J. **98**, 2702–2711
27 Rudolph, B., Podschun, R., Sahly, H., Schubert, S., Schroder, J. M. and Harder, J. (2006) Identification of RNase 8 as a novel human antimicrobial protein. Antimicrob. Agents Chemother. **50**, 3194–3196
27a Torrent, M., Pulido, D., Nogués, M. V. and Boix, E. (2012) Exploring new biological functions of amyloids: bacteria cell agglutination mediated by host protein aggregation. PLoS Pathog. **8**, e1003005
28 Torrent, M., Di Tommaso, P., Pulido, D., Nogues, M. V., Notredame, C., Boix, E. and Andreu, D. (2012) AMPA: an automated web server for prediction of protein antimicrobial regions. Bioinformatics **28**, 130–131
29 Torrent, M., Nogues, M. V. and Boix, E. (2012) Discovering new *in silico* tools for antimicrobial peptide prediction. Curr. Drug Targets **13**, 1148–1157
30 Torrent, M., Andreu, D., Nogues, V. M. and Boix, E. (2011) Connecting peptide physicochemical and antimicrobial properties by a rational prediction model. PLoS ONE **6**, e16968
31 Nguyen, L. T., Haney, E. F. and Vogel, H. J. (2011) The expanding scope of antimicrobial peptide structures and their modes of action. Trends Biotechnol. **29**, 464–472
32 Yeung, A. T., Gellatly, S. L. and Hancock, R. E. (2011) Multifunctional cationic host defence peptides and their clinical applications. Cell. Mol. Life Sci. **68**, 2161–2176
33 D'Errico, G., Ercole, C., Lista, M., Pizzo, E., Falanga, A., Galdiero, S., Spadaccini, R. and Picone, D. (2011) Enforcing the positive charge of N-termini enhances membrane interaction and antitumor activity of bovine seminal ribonuclease. Biochim. Biophys. Acta **1808**, 3007–3015
34 Alvarez-Garcia, E., Martinez-del-Pozo, A. and Gavilanes, J. G. (2009) Role of the basic character of α-sarcin's NH_2-terminal β-hairpin in ribosome recognition and phospholipid interaction. Arch. Biochem. Biophys. **481**, 37–44
35 Wang, H., Schwaderer, A. L., Kline, J., Spencer, J. D., Kline, D. and Hains, D. S. (2013) Contribution of structural domains to the activity of ribonuclease 7 against uropathogenic bacteria. Antimicrob. Agents Chemother. **57**, 766–774
36 Boix, E., Blanco, J. A., Nogues, M. V. and Moussaoui, M. (2013) Nucleotide binding architecture for secreted cytotoxic endoribonucleases. Biochimie **95**, 1087–1097
37 Sikriwal, D., Seth, D. and Batra, J. K. (2009) Role of catalytic and non-catalytic subsite residues in ribonuclease activity of human eosinophil-derived neurotoxin. Biol. Chem. **390**, 225–234
38 Cuchillo, C. M., Nogues, M. V. and Raines, R. T. (2011) Bovine pancreatic ribonuclease: fifty years of the first enzymatic reaction mechanism. Biochemistry **50**, 7835–7841

39 Sneath, P. H. A. and Sokal, R. R. (1973) Numerical Taxonomy. Freeman, San Francisco
40 Zuckerkandl, E. and Pauling, L. (1965) Evolutionary divergence and convergence in proteins. In Evolving Genes and Proteins (Brysol, V. and Vogel, H. J., eds), pp. 97–166, Academic Press, New York
41 Tamura, K, Peterson, D., Peterson, N., Stecher, G., Nei, M. and Kumar, S. (2011) MEGA5: molecular evolutionary genetics analysis using maximum likelihood, evolutionary distance, and maximum parsimony methods. Mol. Biol. Evol. **28**, 2731–2739

Received 5 February 2013/2 July 2013; accepted 20 August 2013
Published as BJ Immediate Publication 20 August 2013, doi:10.1042/BJ20130123

Biochem. J. (2013) **456**, 99–108 (Printed in Great Britain) doi:10.1042/BJ20130123

online data

SUPPLEMENTARY ONLINE DATA

Ribonucleases as a host-defence family: evidence of evolutionarily conserved antimicrobial activity at the N-terminus

Marc TORRENT*†[1,2], David PULIDO*[1], Javier VALLE†, M. Victòria NOGUÉS*, David ANDREU†[2] and Ester BOIX*[2]

*Department of Biochemistry and Molecular Biology, Universitat Autònoma de Barcelona, Cerdanyola del Vallès, 08193 Barcelona, Spain, and †Department of Experimental and Health Sciences, Universitat Pompeu Fabra, Dr. Aiguader 88, 08003 Barcelona, Spain

Sequence similarity in vertebrate secreted RNases

AMPs (antimicrobial peptides/proteins) show similar traits, such as a positive net charge and a high content of hydrophobic amino acids [1]. They are structurally diverse and most of them are unstructured in solution but become structured in the presence of phospholipid membranes and hydrophobic solvents (e.g. TFE). Most AMPs acquire helical structure when present in such hydrophobic environments, but AMPs adopting β-sheet or polyproline helix, or a combination of such secondary structures, have also been described [2]. This heterogeneity makes AMP classification difficult, although several attempts have been made with respectable success [1,3,4]. Although some regular grammars have been proposed for AMPs [5], no general signatures have been outlined, mainly due to their sequence diversity. Although structural signatures like the γ-core motif [6] have been proposed, they are not extendable to all AMPs.

The N-terminal domains of the eight hcRNases fulfil the traits described above. Figure S1 illustrates the low degree of sequence similarity among hcRNases.

Similar results can be observed when aligning representative antimicrobial members of the vertebrate secreted RNase family (Figure S2). Of note, in all cases the net charge and hydrophobicity are similar to those of hcRNases (Table 1 of the main text). Secondary and tertiary structures are also conserved across different species, with all N-terminal domains displaying two α-helices and one β-sheet [7–11]. This sheet structure, however, does not exist in the free form of the hRNase 3 N-terminus [12] where, instead, an extension of the second α-helix has been observed, probably due to increased flexibility at the C-terminus of the domain.

Aggregation and agglutination correlation profiles

Bacterial agglutination is an interesting property in hcRNase 3 that has been correlated with the capacity of the protein to form amyloid-like aggregates [13–15]. These aggregates are indeed important in the cytotoxic mechanism of hcRNase 3. In the present paper we describe a comparable behaviour for all active N-terminal peptides tested, suggesting that this property is not unique to hcRNase 3 but may be shared by all active members of the family.

To investigate whether RNases hold an aggregation-prone N-terminal domain, we have searched for aggregation-prone regions in the N-terminal domains of hRNases using Aggrescan (http://bioinf.uab.es/aggrescan/, Figure S3) [16,17]. In the aggregation plots, all domains have significant segments with positive aggregation values that represent a significant aggregation propensity. The putative region is also shared by other antimicrobial members within the vertebrate RNase family (Figure S4).

As mentioned above, the aggregation propensity of the N-terminal region has been linked to the agglutination behaviour [13,14]. Within this context, we have analysed the potential correlation between the aggregation propensity and the agglutination activity (MAC values, Table 4 of the main text). The results confirm a positive correlation between the two values (Figure S5A), indicating that a high aggregation propensity is required to agglutinate bacteria. A similar correlation between agglutination and hydrophobicity is also observed (Figure S5B).

Peptide structuration and antimicrobial activity

As observed for many AMPs, hcRNase N-termini are poorly structured in solution, but acquire a defined structure in the presence of TFE, SDS or LPS (Figure S6) [12]. However, not all peptides display an equal degree of structuration in those hydrophobic environments. For example, hcRNase 1 is less structured than hcRNase 3 in the presence of SDS or LPS. Interestingly, the degree of structuration in the presence of SDS micelles is correlated with antimicrobial activity (Figure S8A). These results are not surprising as, in general, AMPs acquire α-helix structure upon contact with phospholipid membranes and this step is required for antimicrobial activity [1]. However, peptide structuration is only limited to negatively charged vesicles as no binding is observed for neutral vesicles (Table S1).

Correlation between peptide structuration and membrane action is also evident both *in vivo* and *in vitro*. Indeed, a positive correlation is registered between liposome leakage and bacterial membrane depolarization data (Figure S7). Also relevant is the correlation found for structuration under the presence of LPS micelles and LPS binding (Figure S8B), denoting that similar conclusions apply for the cell-wall structure of Gram-negative bacteria. Even more interesting is the fact that LPS binding also correlates with MIC values (Figure S8C), in accordance with the mechanism suggested for ECP (eosinophil cationic protein) and its N-terminus [18]. Also noteworthy is the fact that ECP has a particularly strong binding for LPS, as well as a high level of structuration in its presence. The structure of N-terminal domain peptides has only been solved for RNase 3 [12] and was found to be similar to the structure of the domain in the protein. As all domains seem to possess a similar structure in the native protein (Figure S9) we do not expect the other peptides to differ from this behaviour, as supported by CD analysis (Figure S6).

[1] These authors contributed equally to this work.

[2] Correspondence may be addressed to any of these authors (email marc.torrent@uab.cat, david.andreu@upf.edu or ester.boix@uab.cat).

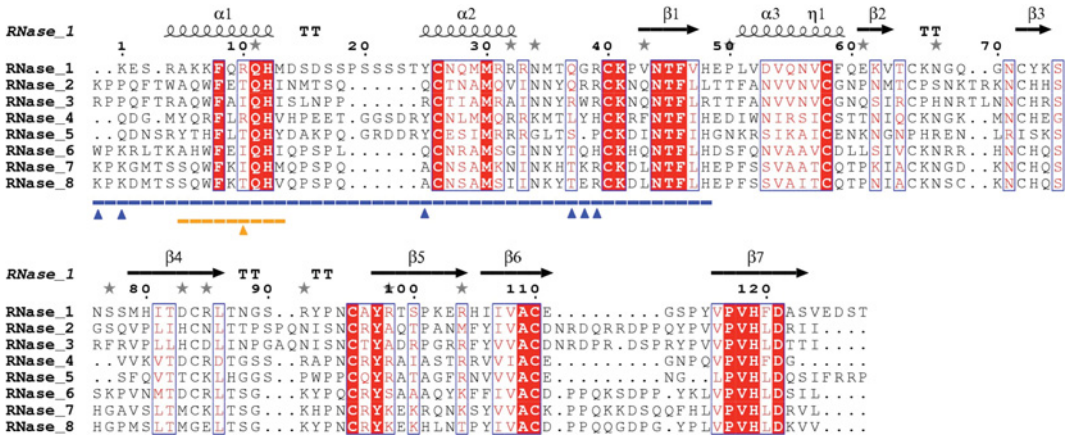

Figure S1 Sequence alignment of hcRNases

Conserved regions are boxed; highly conserved amino acids are coloured in white over a red background, whereas moderately conserved amino acids regions are coloured in red. The secondary structure of hcRNase 3 is displayed as a reference on top of the alignment. The N-terminal antimicrobial domain is highlighted in blue and the agglutination-promoting region in yellow. Arrows denote key residues in both regions.

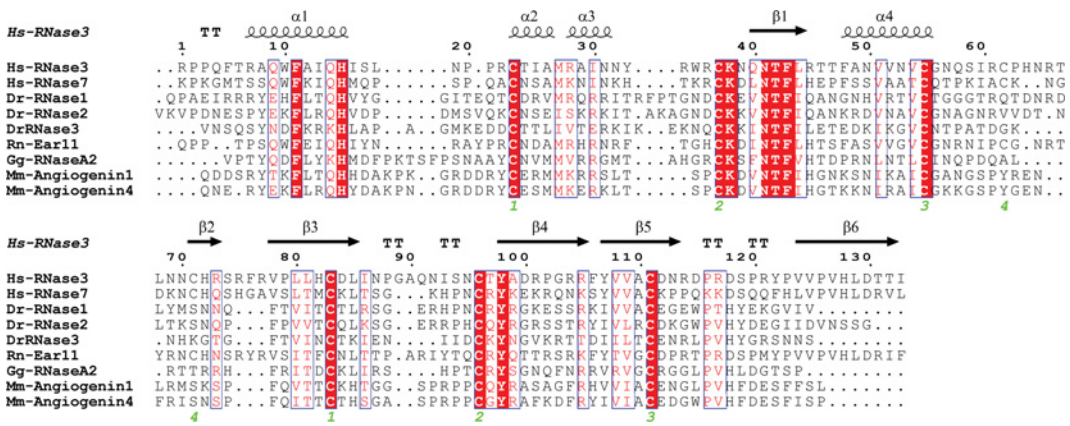

Figure S2 Sequence alignment of several antimicrobial vertebrate RNases

Conserved regions are boxed; highly conserved amino acids are coloured in white over a red background, whereas moderately conserved amino acids regions are coloured in red. The secondary structure of hRNase 3 is displayed as a reference on top of the alignment. Species are *Homo sapiens* (Hs), *Danio rerio* (Dr), *Rattus norvegicus* (Rn), *Gallus gallus* (Gg) and *Mus musculus* (Mm). Ear, eosinophil-associated RNase.

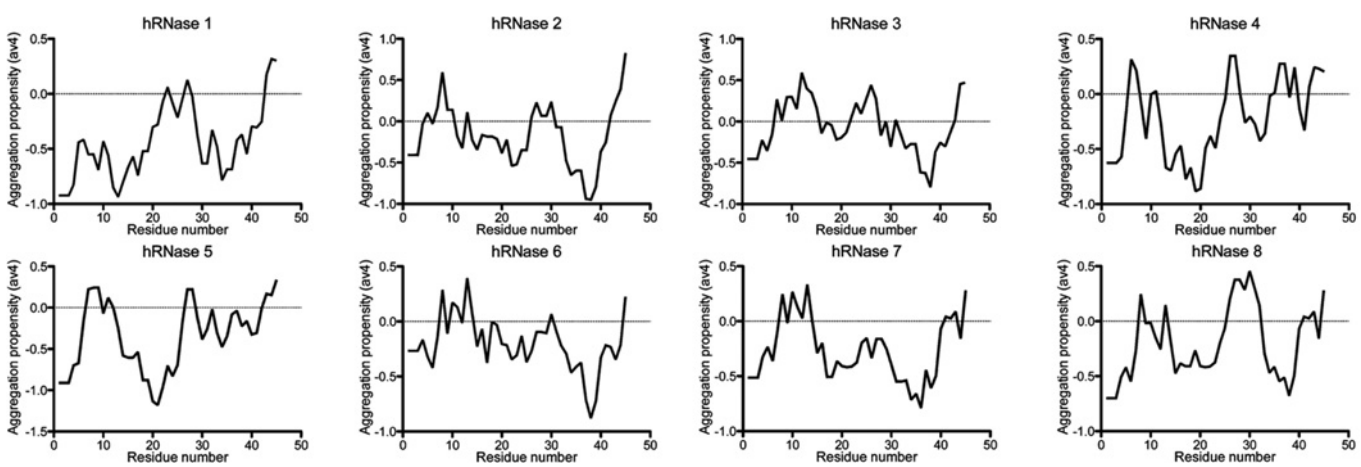

Figure S3 Aggregation profiles for the eight hcRNases

Average aggregation propensity values (av4) are plotted for each amino acid. The hot-spot threshold, marked with a broken line, is defined as the average of multiplying the aggregation propensity values (av4) of each of the 20 natural amino acids by its frequency in the SwissProt database.

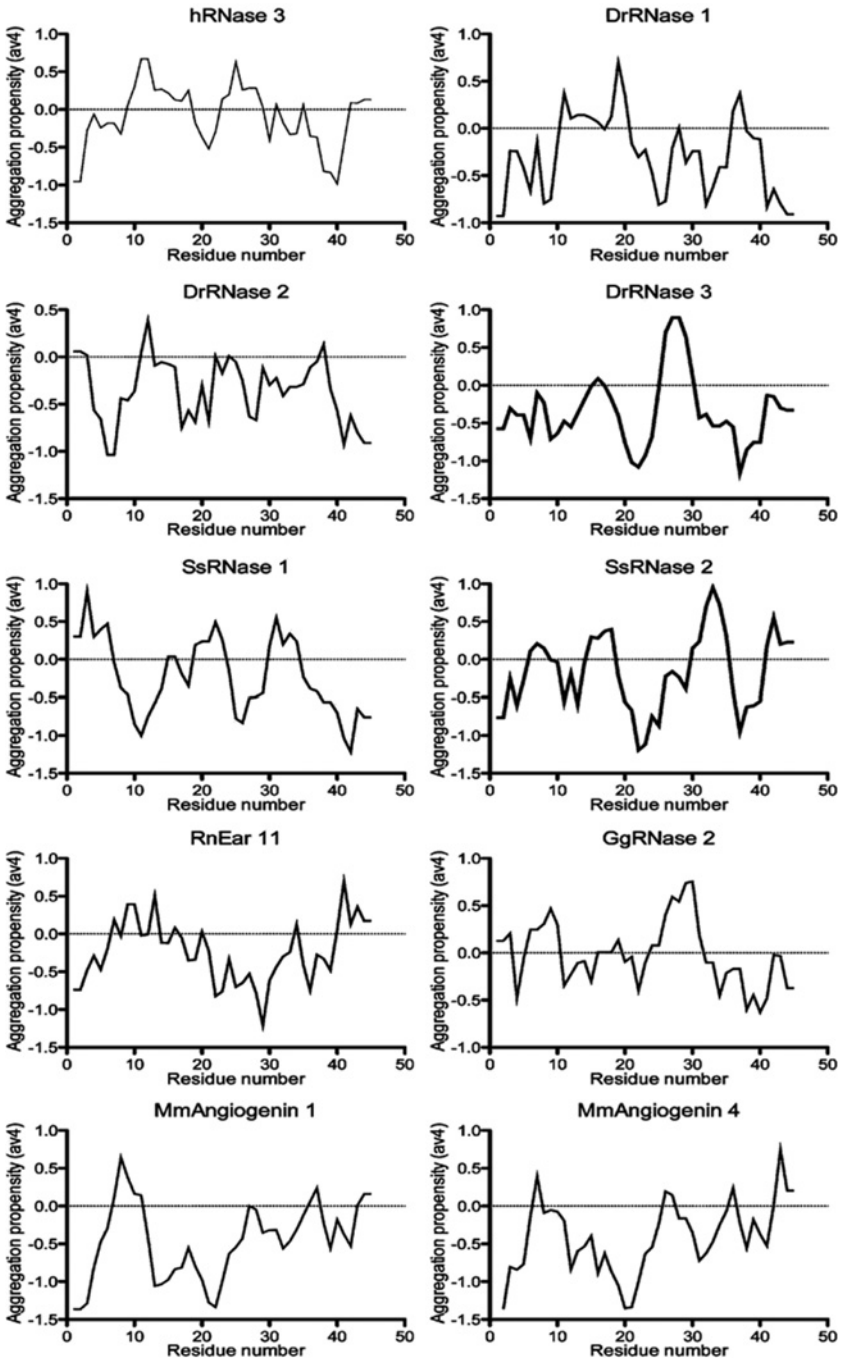

Figure S4 Aggregation profiles for ten well-known antimicrobial vertebrate RNases

Average av4 values are plotted for each amino acid. The hot-spot threshold, as defined for Figure S3, is marked with a broken line. Species are *Salmo salar* (Ss), *Danio rerio* (Dr), *Rattus norvegicus* (Rn), *Gallus gallus* (Gg) and *Mus musculus* (Mm).

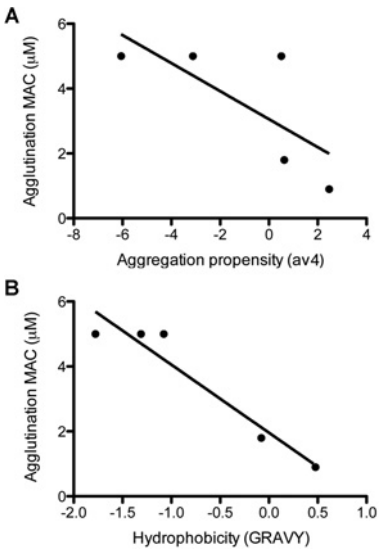

Figure S5 Correlation between agglutination and aggregation in RNase-derived peptides

Agglutinating activity is plotted against aggregation propensity (**A**) and hydrophobicity (**B**). Agglutinating activity is calculated as the MAC value for *E. coli* as shown in Table 4 of the main text. Aggregation propensity and hydrophobicity have been calculated as the average of av4 values (Aggrescan) and hydrophobicity values (GRAVY) for the aggregation-prone region described in RNase 3 (residues 8–16) for each protein in accordance with the sequence alignment (Figure S1).

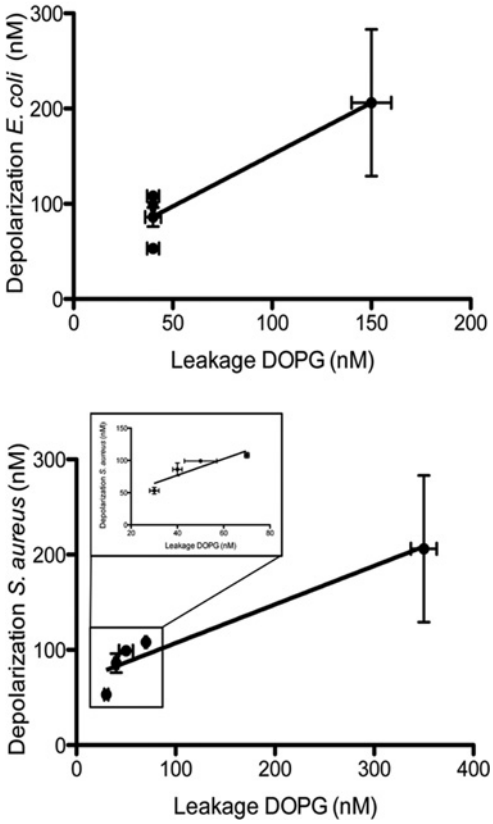

Figure S7 Correlation between bacterial cell depolarization and liposome leakage

Depolarization activity of peptides, calculated using the DiSC assay, is plotted against liposome leakage, evaluated by the ANTS/DPX assay with DOPG LUV (See Tables 3 and 4, and the Materials and methods section in the main text for further information).

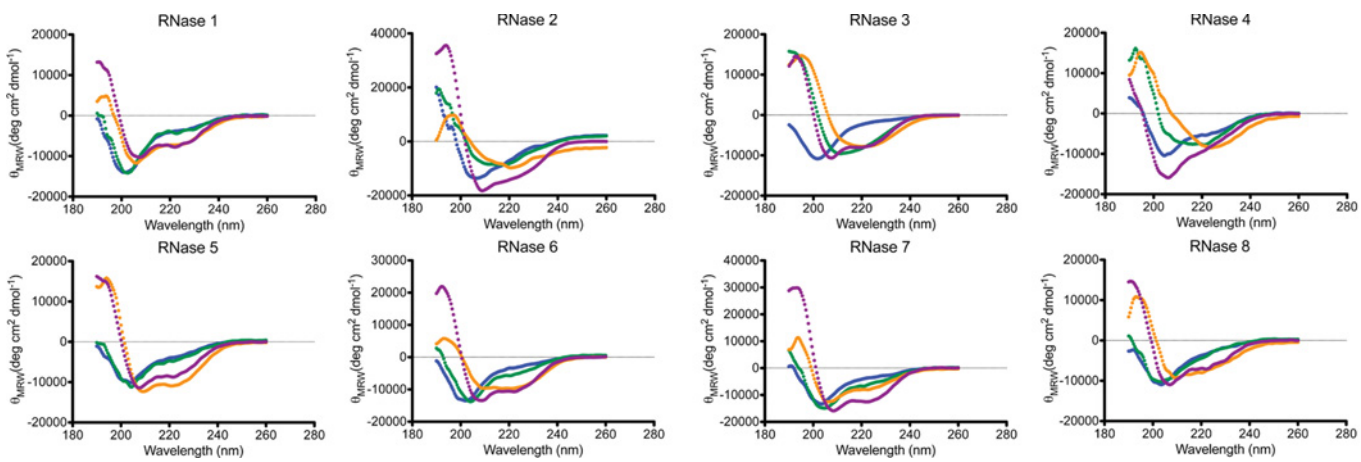

Figure S6 Structural characterization of RNase-derived peptides

CD spectra of peptides 1–8 (corresponding to RNases 1–8) in 5 mM sodium phosphate buffer (pH 7.5) (blue) and in the presence of LPS (green), SDS micelles (orange) and 50 % TFE (purple).

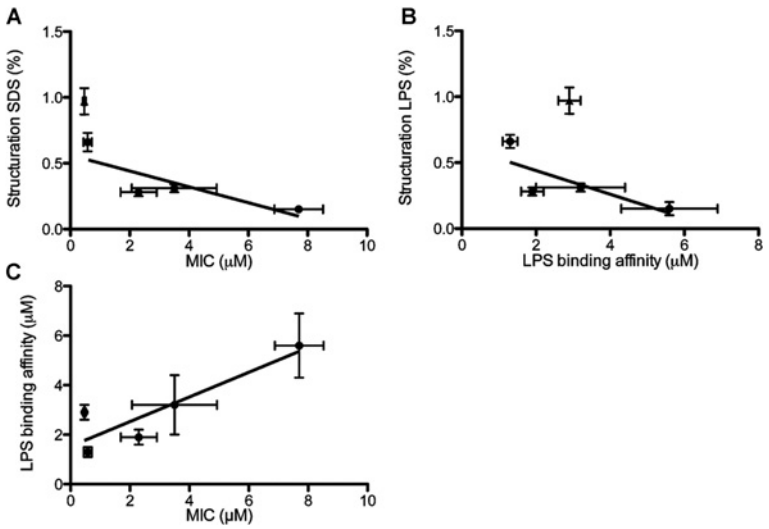

Figure S8 Correlation between biophysical and biological properties in RNase-derived peptides

Structuration in the presence of SDS micelles is plotted against antimicrobial activity (**A**) and LPS-binding affinity (**B**). Also, LPS-binding affinity is plotted against antimicrobial activity (**C**). Antimicrobial activity is expressed as the mean MIC value for all strains in (**A**) and for Gram-negative strains in (**B**). LPS-binding affinity is expressed as EC_{50} (μM), as described in the Materials and methods section of the main text. Peptide structuration is expressed as the percentage of α-helix (measured as θ_{222}) in a given condition with respect to maximum structuration taken as the θ_{222} value in the presence of 50 % TFE.

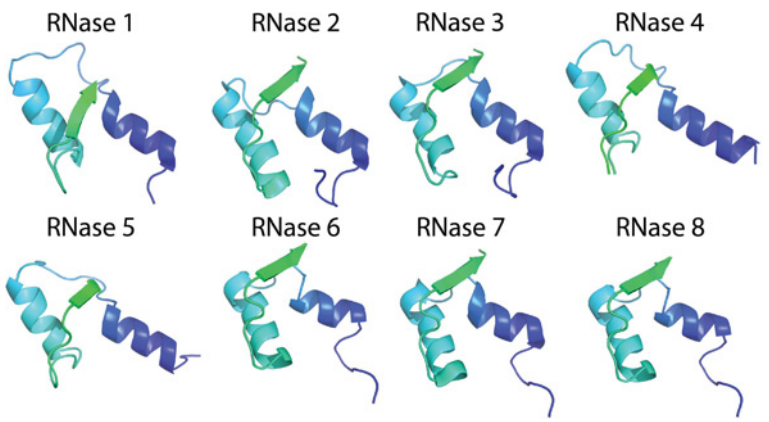

Figure S9 Structure of the N-terminal domains in RNases

Structure of the N-terminal region of RNases. All structures were taken from the PDB database, except RNases 6 and 8 which were obtained using the Swiss Model server (http://swissmodel.expasy.org). PDB codes: RNase 1, 7RSA; RNase 2, 1GQV; RNase 3, 1QMT; RNase 4, 1RNF; RNase 5, 1B1L; and RNase 7, 2HKY.

Table S1 Binding of hcRNase-derived peptides to phospholipid membranes assessed by tryptophan fluorescence spectral analysis

Results are given as λ_{max} (nm). Wavelength of the maximum was measured and calculated as described in [19]. n.a., not applicable.

Peptide	Buffer	DOPC	3:2 DOPC/DOPG	DOPG	LPS	SDS
1	n.a.	n.a.	n.a.	n.a.	n.a.	n.a.
2	351	351	346	345	347	341
3	353	353	344	341	342	341
4	n.a.	n.a.	n.a.	n.a.	n.a.	n.a.
5	n.a.	n.a.	n.a.	n.a.	n.a.	n.a.
6	358	358	349	341	346	340
7	353	353	343	343	343	339
8	n.a.	n.a.	n.a.	n.a.	n.a.	n.a.

Table S2 Antimicrobial activity and biophysical properties (LPS binding and liposome leakage) of lysine and arginine variants of RNase 3 and seven N-terminal peptides respectively

Antimicrobial (MIC_{100}), bacteria agglutination (MAC), haemolytic (HC_{50}), LPS affinity and bacterial leakage assays were performed as described in the Materials and methods section of the main text.

	MIC_{100} (μM)		MAC (μM)			
Peptide	*E. coli*	*S. aureus*	*E. coli*	HC_{50} (μM)	LPS binding (μM)	Leakage (nM)
RNase 3-(1–45)	0.40 ± 0.05	0.40 ± 0.05	1.00 ± 0.10	10.10 ± 1.30	2.60 ± 0.30	93.33 ± 2.24
RNase 3-(1–45)K	0.40 ± 0.05	0.40 ± 0.05	1.00 ± 0.10	9.60 ± 0.50	2.90 ± 0.30	93.31 ± 4.15
RNase 7-(1–45)	1.20 ± 0.20	10.00 ± 1.00	5 ± 0.3	9.73 ± 0.70	3.80 ± 0.40	195.12 ± 2.38
RNase 3-(1–45)R	1.20 ± 0.20	10.00 ± 1.00	5 ± 0.3	9.31 ± 0.70	3.40 ± 0.30	189.67 ± 3.27

REFERENCES

1 Fjell, C. D., Hiss, J. A., Hancock, R. E. and Schneider, G. (2012) Designing antimicrobial peptides: form follows function. Nat. Rev. Drug Discovery **11**, 37–51

2 Nguyen, L. T., Haney, E. F. and Vogel, H. J. (2011) The expanding scope of antimicrobial peptide structures and their modes of action. Trends Biotechnol. **29**, 464–472

3 Hadley, E. B. and Hancock, R. E. (2010) Strategies for the discovery and advancement of novel cationic antimicrobial peptides. Curr. Top. Med. Chem. **10**, 1872–1881

4 Torrent, M., Vogues, M. V. and Boix, E. (2012) Discovering new *in silico* tools for antimicrobial peptide prediction. Curr. Drug Targets **13**, 1148–1157

5 Loose, C., Jensen, K., Rigoutsos, I. and Stephanopoulos, G. (2006) A linguistic model for the rational design of antimicrobial peptides. Nature **443**, 867–869

6 Yeaman, M. R. and Yount, N. Y. (2007) Unifying themes in host defence effector polypeptides. Nat. Rev. Microbiol. **5**, 727–740

7 Acharya, K. R., Shapiro, R., Allen, S. C., Riordan, J. F. and Vallee, B. L. (1994) Crystal structure of human angiogenin reveals the structural basis for its functional divergence from ribonuclease. Proc. Natl. Acad. Sci. U.S.A. **91**, 2915–2919

8 Mosimann, S. C., Newton, D. L., Youle, R. J. and James, M. N. (1996) X-ray crystallographic structure of recombinant eosinophil-derived neurotoxin at 1.83 Å resolution. J. Mol. Biol. **260**, 540–552

9 Huang, Y. C., Lin, Y. M., Chang, T. W., Wu, S. J., Lee, Y. S., Chang, M. D., Chen, C., Wu, S. H. and Liao, Y. D. (2007) The flexible and clustered lysine residues of human ribonuclease 7 are critical for membrane permeability and antimicrobial activity. J. Biol. Chem. **282**, 4626–4633

10 Kover, K. E., Bruix, M., Santoro, J., Batta, G., Laurents, D. V. and Rico, M. (2008) The solution structure and dynamics of human pancreatic ribonuclease determined by NMR spectroscopy provide insight into its remarkable biological activities and inhibition. J. Mol. Biol. **379**, 953–965

11 Laurents, D. V., Bruix, M., Jimenez, M. A., Santoro, J., Boix, E., Moussaoui, M., Nogues, M. V. and Rico, M. (2009) The ^{1}H, ^{13}C, ^{15}N resonance assignment, solution structure, and residue level stability of eosinophil cationic protein/RNase 3 determined by NMR spectroscopy. Biopolymers **91**, 1018–1028

12 Garcia-Mayoral, M. F., Moussaoui, M., de la Torre, B. G., Andreu, D., Boix, E., Nogues, M. V., Rico, M., Laurents, D. V. and Bruix, M. (2010) NMR structural determinants of eosinophil cationic protein binding to membrane and heparin mimetics. Biophys. J. **98**, 2702–2711

13 Torrent, M, Badia, M., Moussaoui, M., Sanchez, D., Nogues, M. V. and Boix, E. (2010) Comparison of human RNase 3 and RNase 7 bactericidal action at the Gram-negative and Gram-positive bacterial cell wall. FEBS J. **277**, 1713–1725

14 Torrent, M., Odorizzi, F., Nogues, M. V. and Boix, E. (2010) Eosinophil cationic protein aggregation: identification of an N-terminus amyloid prone region. Biomacromolecules **11**, 1983–1990

15 Torrent, M., Pulido, D., Nogues, M. V. and Boix, E. (2012) Exploring new biological functions of amyloids: bacteria cell agglutination mediated by host protein aggregation. PLoS Pathog. **8**, e1003005

16 Conchillo-Sole, O., de Groot, N. S., Aviles, F. X., Vendrell, J., Daura, X. and Ventura, S. (2007) AGGRESCAN: a server for the prediction and evaluation of "hot spots" of aggregation in polypeptides. BMC Bioinf. **8**, 65

17 de Groot, N. S., Castillo, V., Grana-Montes, R. and Ventura, S. (2012) AGGRESCAN: method, application, and perspectives for drug design. Methods Mol. Biol. **819**, 199–220

18 Torrent, M., de la Torre, B. G., Nogues, V. M., Andreu, D. and Boix, E. (2009) Bactericidal and membrane disruption activities of the eosinophil cationic protein are largely retained in an N-terminal fragment. Biochem. J. **421**, 425–434

19 Torrent, M., Cuyas, E., Carreras, E., Navarro, S., Lopez, O., de la Maza, A., Nogues, M. V., Reshetnyak, Y. K. and Boix, E. (2007) Topography studies on the membrane interaction mechanism of the eosinophil cationic protein. Biochemistry **46**, 720–733

Received 5 February 2013/2 July 2013; accepted 20 August 2013
Published as BJ Immediate Publication 20 August 2013, doi:10.1042/BJ20130123